J Appl Electrochem (2007) 37:1345–1355
DOI 10.1007/s10800-007-9394-1

ORIGINAL PAPER

Time averaged temperature calculations in pulse electrochemical machining. Part I: theoretical basis

N. Smets · S. Van Damme · D. De Wilde · G. Weyns · J. Deconinck

Received: 7 March 2007 / Revised: 26 July 2007 / Accepted: 27 July 2007 / Published online: 28 August 2007

Abstract Simulation of the temperature distribution during the Pulse Electrochemical Machining (PECM) process provides information on system design and guidelines for practical use. The pulses that are applied to the PECM system have to be described on a time scale that can be orders of magnitude smaller than the time scale on which the thermal effects evolve. If the full detail of the applied pulses has to be taken into account, the time accurate calculation of the temperature distribution in PECM can become a computationally very expensive procedure. A new approach is introduced by time averaging the heat sources of the system. Performing this, the time steps used during the calculations are no longer dictated by the pulse characteristics. Using this approach, computationally very cheap, yet satisfactory results can be obtained. In this part of the work, the hybrid calculation and the Quasi Steady State ShortCut (QSSSC) are introduced. The hybrid calculation is a method, by which averaged and pulsed heat sources are combined in one calculation. The QSSSC is a method for quickly calculating the Quasi Steady State (QSS) in numerical calculations with time stepping. Analytical solutions of simplified cases are studied to provide useful insights into the more general case. It is shown that the averaging technique adopted in this work does not always deliver perfect results. However, using a technique of shifting the pulses in time, the results can become very satisfactory yet still extremely cheap. The more general case, which will be solved numerically, can be found in part II [Smets et al. J Appl Electrochem (Submitted)] of this work.

Keywords Pulse electrochemical machining · Temperature distribution · Time averaging · Transient

Notation

A	Electrode surface (m^2)
Bi	Biot Number ($=\frac{hH}{k}$)
C_p	Heat capacity (J kg^{-1} K^{-1})
Fo	Fourier Number ($=\frac{\alpha' t}{H^2}$)
h	Heat transfer coefficient (W m^{-2} K^{-1})
H	Characteristic size electrode (m)
j	Current density (A m^{-2})
k	Thermal conductivity (W m^{-1} K^{-1})
L	Electrode length (m)
P_{dl}	Heat density produced in the double layer (W m^{-2})
P_{bulk}	Heat density produced in the bulk (W m^{-3})
$\overline{r}$	General location vector (m)
St	Strouhal Number ($=\frac{L}{vT}$)
t	Time (s)
t'	Time (s)
λ	Time (s)
T	Pulse period (s)
v	Scalar velocity (m s^{-1})
$\overline{v}$	Velocity vector (m s^{-1})
V	Volume (m^3)
x	Distance (m)
α	Duty cycle
α'	Thermal diffusivity (m^2 s^{-1})
η	Overpotential (V)
θ	Relative temperature (K)
θ'	Normalized temperature (K)
$\overline{\theta}$	Averaged temperature (K)

N. Smets (✉) · S. Van Damme · D. De Wilde · G. Weyns · J. DeconinckVrije Universiteit Brussel IR/ETEC, Pleinlaan 2, Brussels 1050, Belgium
e-mail: nsmets@vub.ac.be

$\tilde{\theta}$	Temperature ripple (K)
θ_{decay}	Decaying temperature (K)
Θ	Temperature (K)
Θ_{init}	Initial temperature (K)
Θ_{∞}	Reference temperature (K)
Θ^{*}	Steady state temperature (K)
$\hat{\lambda}_n$	Transcendental coefficients
ρ	Density (kg m^{-3})
σ	Electrical conductivity (S m^{-1})
τ	Time constant (s)
ψ	Pulse delay (s)

1 Introduction

Electrochemical Machining (ECM) is a manufacturing process based on the controlled anodic dissolution of a metal at large current densities (in the region of 1 A mm^{-2}). An electrolyte is used to carry away produced heat, among other reaction products.

Despite its advantages, some difficulties still trouble the application of ECM. One important issue is the lack of quantitative simulation software to predict the tool shape and machining parameters necessary to produce a given work-piece profile [2–4]. The most complete model needs to deal with the effects of the fluid flow, gas evolution, heat generation, the electrochemical processes at the electrodes, the transport of the species involved and all this while the electrode shape changes. The work reported here makes a contribution in incorporating heat generation in the model and calculating the temperature distributions.

Pulse Electrochemical Machining (PECM) involves the application of current or voltage pulses. In this work, only current pulses will be considered. This does not compromise the generality, since voltage and current are closely related. One wishes to apply pulsed current for reasons of accuracy and surface quality [4–7]. The issue of heating of the electrolyte is of primary importance for the determination of the limiting conditions in ECM [6–10].

Steady State (SS) temperature distribution calculations have been performed by Clark and McGeough [9], Loutrel and Cook [10] and Kozak et al. [8]. Time accurate calculations of temperature distribution during PECM have already been performed by Kozak [5, 6], where the pulses are considered to be independent of each other and thus no accumulation of heat over multiple periods is encountered. Cases where there was accumulation of heat in the system during multiple pulses have been treated in previous work of the authors [11]. It was shown that, in order to determine in advance whether the heat produced during multiple pulses is going to accumulate or not, the time scales present in the system have to be studied.

To simulate electrochemical processes with current pulses, one has to perform calculations with boundary conditions that vary in time. By applying a time stepping algorithm, all the variable distributions are calculated in time. The applied pulses have to be described on a time scale that can be orders of magnitude smaller than the time scale on which the thermal effects evolve. This means that a lot of time steps would have to be calculated to perform a satisfactory thermal simulation, which would be a computationally very expensive procedure. The aim of this paper was to find a cheaper approach that would still provide adequate predictions.

By averaging the heat production in the system, it is possible to calculate temperature evolutions with time steps that are not dictated by the time scale of the pulses. It also provides the possibility of calculating a SS. However, plain averaging is inadequate in the system under consideration, because of the very broad spectrum of possible time scales present (see also [11]). While averaging might be necessary to handle the largest time scales, the smaller time scales may still be very important relative to the pulse period. Plain averaging would eliminate all the small time scale effects, which would make it impossible to perform accurate simulations. The hybrid calculation and the Quasi Steady State ShortCut (QSSSC) are introduced in this work as a solution to this problem. The hybrid calculation is a method where initially averaged heat sources are applied, and at the time of interest, pulsed heat sources are applied. The QSSSC consists of using the averaged SS as a starting state, and applying pulses afterwards. It is shown that delaying the start of the pulse on-time, with a certain value ψ, influences the accuracy of the approximate methods. Analytical formulae for ψ are presented in this work. Also, a function E is defined to quantify how well the QSS is approximated by using the QSSSC.

2 Mathematical model

The temperature distribution in the system is calculated using a convection–diffusion equation with heat sources:

$$\rho C_p \frac{\partial \Theta}{\partial t} + \rho C_p \overline{v} \cdot \overline{\nabla} \Theta = \overline{\nabla} \cdot \left(k \overline{\nabla} \Theta \right) + P_{\text{bulk}} \tag{1}$$

Joule heating in the bulk of both the electrolyte and the electrodes is considered, where

$$P_{\text{bulk}} = \frac{j^2}{\sigma} \tag{2}$$

Heat dissipation in the double layer, where [10]

$$P_{\text{dl}} = \eta j \tag{3}$$

is also taken into account. P_{dl} is imposed as a heat flux at the electrode surfaces that are the boundaries of two domains: the electrodes and the electrolyte. The electrodes are cooled by convection. The boundaries of the electrodes, which are not contiguous to the electrolyte, are considered thermal insulators. This choice is justified by the fact that essentially all of the heat generated in the system must be carried away by the electrolyte [10].

3 Time averaging

Strongly time dependent pulsating boundary conditions and bulk sources require simulations using small timesteps. However, it would be more convenient to apply constant boundary conditions and bulk sources, such that the time-steps would not be dictated by the time scale of the pulses, and that SS calculations would be possible. One way to achieve this, is by averaging the boundary conditions and bulk sources in time.

A time averaging operator $\langle\cdot\rangle$ can be defined as

$$\langle\varphi(t)\rangle = \frac{1}{T}\int_{t-T+\Gamma}^{t+\Gamma}\varphi(\lambda)\mathrm{d}\lambda \tag{4}$$

where averaging is performed over one period T, and where Γ provides the freedom of placing the integration interval around t in an arbitrary way. The averaged quantity is undefined in the first $T-\Gamma$ and the last Γ of the time interval under consideration, which will be neglected. The average heat production in the double layer can be calculated easily from the heat production during the on-time of the pulse $P_{dl,on}(\overline{r})$, as

$$\langle P_{dl}(\overline{r},t)\rangle = \alpha P_{dl,on}(\overline{r}) \tag{5}$$

Averaging the bulk heat production in time gives

$$\langle P_{bulk}(\overline{r},t)\rangle = \alpha P_{bulk,on}(\overline{r}) \tag{6}$$

with $P_{bulk,on}(\overline{r})$ the bulk heat production during the on-time of the pulse.

4 Averaging analytical solutions of simplified problems

In order to be able to justify the concept of averaging, simplified models are analyzed. Interesting conclusions will be drawn here which will be extrapolated to the more general case that will be solved numerically. Two sub-systems are considered: conduction in the electrode, and convection in the electrolyte.

4.1 Conduction in the electrode

One electrode is considered in this system. Heat density $P_{dl}(t)$ will be produced at the contact surface with the electrolyte. Heat production in the electrode will be neglected, because of the typically very high electrical conductivity of the metal electrodes and hence the very low heat production. The electrode is cooled by convection. The thermal behaviour of the electrode is studied for a simplified case, and a more general case in the following sections.

4.1.1 Lumped capacity solution

If the assumption is valid that the electrode is always at a uniform temperature $\Theta(t)$, a lumped capacity solution can be used. This assumption is valid if the Biot number [12] is much smaller than one,

$$Bi = \frac{hH}{k} \ll 1 \tag{7}$$

for which $H = V/A$ is taken. This case of the lumped capacity solution will be given as a step to the more general case, which is treated later in Sect. 4.1.2.

Part of the produced heat $P_{dl}(t)$ will be removed by the electrolyte, and the other part will heat up the electrode. The following equation applies,

$$hA(\Theta(t)-\Theta_\infty) + \rho C_p V\frac{\mathrm{d}\Theta(t)}{\mathrm{d}t} = P_{dl}(t)A \tag{8}$$

which can be rewritten as

$$hA(\Theta(t)-\Theta^*(t)) + \rho C_p V\frac{\mathrm{d}\Theta(t)}{\mathrm{d}t} = 0 \tag{9}$$

with $\Theta^*(t) = P_{dl}(t)/h + \Theta_\infty$. This shows that the system, in which there is convective cooling into a medium at temperature Θ_∞ with a heat transfer coefficient h and simultaneous heating $P_{dl}(t)$ at the interface, is actually equivalent to the same system being heated by convection by a medium at temperature $\Theta^*(t)$. The latter situation will be considered in the rest of this work for easier formulation.

From the absolute temperature Θ the relative temperature θ can be derived, using

$$\theta(t) = \Theta(t) - \Theta_\infty \tag{10}$$

Using the initial condition $\Theta(0) - \Theta_\infty = \theta_{init}$, the solution of Eq. 9, for $P_{dl}(t) = P_{dl}$ constant, is

$$\theta(t) = \theta^* - (\theta^* - \theta_{init})e^{-\frac{t}{\tau}} \tag{11}$$

with time constant $\tau = \rho C_p H/h$, SS temperature $\theta^* = P_{dl}/h$, and initial temperature θ_{init}.

If $P_{dl}(t)$ is a pulse train in time, and alternates between a certain value $P_{dl,on}$ and zero, $\theta(t)$ will be a chaining of exponential courses (see Fig. 1a). The boundary condition is then defined in time as

$$\theta^*(t) = \begin{cases} 0 & \text{for } t' < 0 \\ \theta^* & \text{for } iT \le t' < iT + \alpha T, \quad \text{on-time,} \\ 0 & \text{for } iT + \alpha T \le t' < (i+1)T, \quad \text{off-time,} \end{cases} \tag{12}$$

with $i = 0, 1, 2,...$ the number of the period. To provide a degree of freedom which will be exploited later, the time t', which lags ψ to t, is introduced

$$t' = t - \psi \tag{13}$$

The solution of Eq. 9 with boundary condition 12 and initial condition $\theta_{init} = 0$ is the following recursive formulation,

$$\theta(t) = \begin{cases} 0 & \text{for } t' \le 0, \\ \theta^* - (\theta^* - \theta(iT))e^{-(t'-iT)/\tau} & \text{on-time,} \\ \theta(iT + \alpha T)e^{-(t'-(iT+\alpha T))/\tau} & \text{off-time,} \end{cases} \tag{14}$$

where the start temperature of one piece is the end temperature of the previous piece. Fortunately, a more convenient general formulation can be found,

$$\frac{\theta(t)}{\theta^*} = \begin{cases} 0, & \text{for } t' \le 0, \\ 1 - \frac{e^{T/\tau} - e^{\alpha T/\tau}}{e^{T/\tau}-1} e^{-(t'-iT)/\tau} - \frac{e^{\alpha T/\tau}-1}{e^{T/\tau}-1} e^{-t'/\tau}, & \text{on-time,} \\ \frac{e^{-\alpha T/\tau}-1}{e^{-T/\tau}-1} e^{-(t'-iT-\alpha T)/\tau} - \frac{e^{\alpha T/\tau}-1}{e^{T/\tau}-1} e^{-t'/\tau}, & \text{off-time.} \end{cases} \tag{15}$$

The last term in the equations of solution 15 is a transient term which vanishes for $t \to \infty$. The solution then converges to the QSS temperature evolution,

$$\frac{\theta_{QSS}(t)}{\theta^*} = \begin{cases} 1 - \frac{e^{T/\tau} - e^{\alpha T/\tau}}{e^{T/\tau}-1} e^{-(t'-iT)/\tau}, & \text{on-time,} \\ \frac{e^{-\alpha T/\tau}-1}{e^{-T/\tau}-1} e^{-(t'-iT-\alpha T)/\tau}, & \text{off-time.} \end{cases} \tag{16}$$

By subtracting its average value from $\theta_{QSS}(t)$, $\theta^*_{av} = \alpha\theta^*$, the ripple $\tilde{\theta}(t)$ is obtained,

$$\begin{aligned} \tilde{\theta}(t) &= \theta_{QSS}(t) - \langle \theta_{QSS}(t) \rangle \\ &= \theta_{QSS}(t) - \theta^*_{av} \end{aligned} \tag{17}$$

which has an average value of zero. $\tilde{\theta}(t) = 0$ for $t < 0$.

The mathematically more rigorous method for calculating the averaged temperature would be by applying the averaging operator (Eq. 4) on Eq. 9, which yields,

$$\langle \theta(t) \rangle = \theta^*_{av} - \frac{\tau}{T}(\theta(t + \Gamma) - \theta(t - T + \Gamma)) \tag{18}$$

Using Eq. 15 the following averaged temperature is obtained,

$$\langle \theta(t) \rangle = \theta^*_{av} - \theta^* \frac{\tau}{T}(e^{\alpha T/\tau} - 1)e^{-(t'+\Gamma)/\tau} \tag{19}$$

By varying Γ, $\langle \theta(t) \rangle$ can be shifted in time. By choosing for example

$$\Gamma = \psi + \tau \ln\left(\frac{e^{\alpha T/\tau} - 1}{\alpha T/\tau}\right) \tag{20}$$

one obtains

$$\langle \theta(t) \rangle = \theta^*_{av} - \theta^*_{av} e^{-t/\tau} \tag{21}$$

A more pragmatic method with the same result would involve calculating a DC case with the averaged heat production applied. This yields

$$\overline{\theta}(t) = \theta^*_{av} - (\theta^*_{av} - \theta_{init})e^{-t/\tau} \tag{22}$$

where the shorter notation $\overline{\theta}(t) = \langle \theta(t) \rangle$ is used. The latter method is much easier to perform and hence was adopted for the rest of this work. For time shifting between the averaged temperature evolution $\overline{\theta}(t)$ and the pulsed temperature evolution $\theta(t)$, only the parameter ψ will be used.

A decaying contribution $\theta_{decay}(t)$ is defined by stating the following decomposition of the temperature evolution,

$$\theta(t) = \overline{\theta}(t) + \tilde{\theta}(t) + \theta_{decay}(t) \tag{23}$$

and can be calculated as

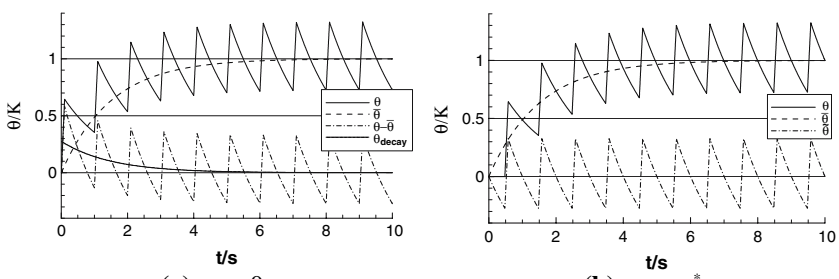

Fig. 1 Temperature evolutions of the lumped capacity solution, electrode initially at electrolyte temperature ($\theta_{init} = 0$)

(a) $\psi = 0$. **(b)** $\psi = \psi^*$.

$$\frac{\theta_{\text{decay}}(t)}{\theta^*} = \left(\alpha - \frac{e^{\alpha T/\tau}-1}{e^{T/\tau}-1}e^{\psi/\tau}\right)e^{-t/\tau} \tag{24}$$

$\theta_{\text{decay}} = 0$ for $t < 0$. By choosing ψ equal to the value

$$\psi^* = \tau \ln\left(\alpha\frac{e^{T/\tau}-1}{e^{\alpha T/\tau}-1}\right) \tag{25}$$

$\theta_{\text{decay}} = 0$ can be made exactly zero. In cases where $T \ll \tau$, Eq. 25 simplifies to

$$\psi^* \approx \frac{(1-\alpha)T}{2} \tag{26}$$

It is possible to combine the averaged boundary conditions and pulses in one calculation. These calculations will be called hybrid. Starting from $t = 0$, the averaged heat sources are applied, and after time $t = t^*$, pulses are applied (possibly delayed by ψ). It can be shown that the temperature evolution is composed of the averaged component $\overline{\theta}(t)$, and a ripple $\tilde{\theta}(t-t^*)$ and a decaying component $\theta_{\text{decay}}(t-t^*)$ starting from the time $t = t^*$:

$$\theta_{\text{hybrid}}(t) = \overline{\theta}(t) + \tilde{\theta}(t-t^*) + \theta_{\text{decay}}(t-t^*) \tag{27}$$

A particularly interesting case is when $t^* \to \infty$. The starting state at $t = t^*$ is then the averaged SS. This situation is called the QSSSC. When performing the QSSSC it is convenient to start the pulsed calculation from $t = 0$, while applying the averaged SS as initial state. In this case, the averaged temperature reduces to $\overline{\theta}(t) = \theta^*_{\text{av}}$:

$$\theta_{\text{QSSSC}}(t) = \theta^*_{\text{av}} + \tilde{\theta}(t) + \theta_{\text{decay}}(t) \tag{28}$$

To clarify the formulae obtained previously a few examples are given. For these $\tau = 1.5$ s, $T = 1$ s, $\alpha = 0.1$ and $\theta^* = 10$ K are taken. The electrode is initially at electrolyte temperature, $\theta_{\text{init}} = 0$. For $\psi = 0$ the temperature evolution is given in Fig. 1a, and for $\psi = \psi^*$ the temperature evolution is given in Fig. 1b. It can be seen that in the case where $\psi = 0, \theta(t) - \overline{\theta}(t) = \tilde{\theta}(t) + \theta_{\text{decay}}(t)$ is clearly composed of a ripple and a decaying contribution. In the case where $\psi = \psi^*$, the decaying contribution $\theta_{\text{decay}}(t)$ is zero, and hence the averaged temperature is equal to the average of $\theta(t)$, $\overline{\theta}(t) = \langle\theta(t)\rangle$.

In the next two examples, the QSSSC will be performed, and hence the electrode is initially at the SS temperature of the averaged case, $\theta_{\text{init}} = \theta^*_{\text{av}}$. In the case where $\psi = 0$, there is a decaying contribution present in $\theta(t)$ before the QSS is reached (Fig. 2a). In the case where $\psi = \psi^*$, the QSS is reached immediately (Fig. 2b), without a further transient.

The analysis in this work is performed on analytical solutions, but the resulting conclusions are intended for application on time stepping calculations. In the case of an analytical solution, it is possible to calculate the QSS straight away. However, during numerical calculations the QSS needs to be obtained through time stepping, which very often involves calculating through some history. In this case, the QSSSC is a very useful tool to minimize or even totally avoid this history (see Fig. 2b). Hence the QSS can be computed with a minimum of timesteps.

4.1.2 Transient conduction in a 1D slab

In ECM, the flow velocities are typically relatively high, giving rise to high convection coefficients h and hence high Biot numbers. In such cases, the lumped capacity solution is not valid. Transient conduction in a 1D slab is described in the literature; if the slab is cooled by convection with a constant convection coefficient h, the solution is [12]

$$\theta' = \sum_{n=1}^{\infty} e^{-\hat{\lambda}_n^2 Fo}\frac{2\sin\hat{\lambda}_n}{\hat{\lambda}_n + \sin\hat{\lambda}_n\cos\hat{\lambda}_n}\cos\left(\hat{\lambda}_n\frac{x}{H}\right) \tag{29}$$

where $Fo = \frac{\alpha' t}{H^2}$ and $\alpha' = \frac{k}{\rho C_p}$. Starting from the side which is insulated, the distance x is measured and $\theta' = \frac{\Theta-\Theta^*}{\Theta_{\text{init}}-\Theta^*}$. The coefficients $\hat{\lambda}_n$ are the successive roots of the transcendental equation

$$\cot\hat{\lambda}_n = \frac{\hat{\lambda}_n}{Bi} \tag{30}$$

For $Fo > 0.2$ the series from Eq. 29 may be approximated using only their first term

$$\theta' \approx A_1\cos\left(\hat{\lambda}_1\frac{x}{H}\right)e^{-\hat{\lambda}_1^2 Fo} \tag{31}$$

with A_1 and $\hat{\lambda}_1$ conveniently tabulated as a function of the Biot number [12].

Duhamel's theorem [13] relates the solution of problems with time-dependent boundary conditions to the solution of reduced problems with time-independent boundary conditions (Eq. 29). The solution with pulsating heat production at the surface of the electrode, and hence with the boundary condition described in Eq. 12, is found to be

$$\frac{\theta(x,t')}{\theta^*} = \begin{cases} 0, & \text{for } t' \le 0 \\ \sum_{k=1}^{\infty}\beta_k(x)\left[1 - \frac{e^{T/\tau_k}-e^{\alpha T/\tau_k}}{e^{T/\tau_k}-1}e^{-(t'-iT)/\tau_k}\right. & \text{on-time} \\ \qquad \left. - \frac{e^{\alpha T/\tau_k}-1}{e^{T/\tau_k}-1}e^{-t'/\tau_k}\right], & \\ \sum_{k=1}^{\infty}\beta_k(x)\left[\frac{e^{-\alpha T/\tau_k}-1}{e^{-T/\tau_k}-1}e^{-(t'-iT-\alpha T)/\tau_k}\right. & \text{off-time} \\ \qquad \left. - \frac{e^{\alpha T/\tau_k}-1}{e^{T/\tau_k}-1}e^{-t'/\tau_k}\right], & \end{cases} \tag{32}$$

with

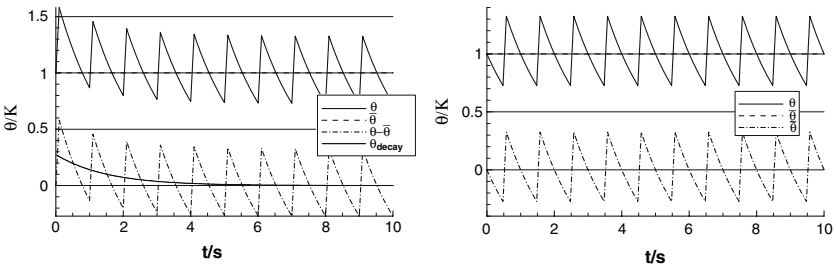

Fig. 2 Temperature evolutions of the lumped capacity solution, electrode initially at averaged SS temperature ($\theta_{init} = \theta^*_{av}$)

(a) $\psi = 0$. **(b)** $\psi = \psi^*$.

$$\beta_k(x) = \frac{2\sin\hat{\lambda}_k}{\hat{\lambda}_k + \sin\hat{\lambda}_k\cos\hat{\lambda}_k}\cos\left(\hat{\lambda}_k\frac{x}{H}\right) \tag{33}$$

and

$$\tau_k = \frac{H^2}{\alpha'\hat{\lambda}_k^2} \tag{34}$$

where $\hat{\lambda}_k$ are the successive roots of the transcendental Eq. 30. Note that

$$\sum_{k=1}^{\infty}\beta_k(x) = 1 \tag{35}$$

A strong similarity can be noted between formulae 32 and 15. The temperature evolution expressions of Sect. 4.1.1 for the lumped capacity solution can be reused in this section for the 1D slab by taking the right hand side of the formulae, placing $\sum_{k=1}^{\infty}\beta_k(x)$ in front of them and replacing τ by τ_k. This operation is valid for Eqs. 15, 16 and 22; Eq. 17 remains valid.

The decompositions of the temperature evolutions are now

$$\theta(x,t) = \overline{\theta}(x,t) + \tilde{\theta}(x,t) + \theta_{decay}(x,t) \tag{36}$$

$$\theta_{hybrid}(x,t) = \overline{\theta}(x,t) + \tilde{\theta}(x,t-t^*) + \theta_{decay}(x,t-t^*) \tag{37}$$

$$\theta_{QSSSC}(x,t) = \theta^*_{av} + \tilde{\theta}(x,t) + \theta_{decay}(x,t) \tag{38}$$

and the expression for $\theta_{decay}(x,t)$ becomes

$$\frac{\theta_{decay}(x,t)}{\theta^*} = \sum_{k=1}^{\infty}\beta_k(x)\left(\alpha - \frac{e^{\alpha T/\tau_k}-1}{e^{T/\tau_k}-1}e^{\psi/\tau_k}\right)e^{-t/\tau_k} \tag{39}$$

Expression 39 cannot be made exactly zero by the choice of the one degree of freedom ψ. The component for which $k = 1$, will be made zero. This component is not necessarily the largest in amplitude, but it is always the slowest one to damp out. The following value for ψ^* is obtained:

$$\psi^* = \tau_1 \ln\left(\alpha\frac{e^{T/\tau_1}-1}{e^{\alpha T/\tau_1}-1}\right) \tag{40}$$

A perfect jump straight into the QSS as in Sect. 4.1.2 is not possible here. This was to be expected, since the result of the SS calculation is a body at uniform temperature, and such a state is never encountered during the QSS. Hence, a transient must occur to step into the QSS starting from the SS.

The transient temperature evolution, together with the QSSSC, is calculated for a case where $x/H = 0$, $\alpha = 0.1$, $T' = 0.3$ and $Bi = 10$. By not delaying the pulses in time, the results from Fig. 3 are obtained. By delaying the pulses with ψ^*, the results from Fig. 4 are obtained. It can be seen that by delaying the pulses with ψ^*, $\theta_{decay}(x,t)$, can be reduced strongly.

In the DC solution, it takes until about $Fo = 0.2$ for the higher order components in the solution to pass. When delaying the pulses with ψ^*, these higher order components are all still present in $\theta_{decay}(x,t)$. The higher order components in $\theta_{decay}(x,t)$ are also a function of T. When T becomes small, $\theta_{decay}(x,t)$ will also become small more quickly, which is very convenient because it keeps the undesirable $\theta_{decay}(x,t)$ under control.

The impact of the undesirable $\theta_{decay}(x,t)$ will be quantified from here. Only the QSSSC will be studied. The other methods contain the same $\theta_{decay}(x,t)$. The smaller $\theta_{decay}(x,t)$, the more accurate the QSSSC approximates the real QSS. The difference between the QSSSC and the QSS, will be quantified with the function E (in %), which is defined as

$$\begin{aligned} E_j &= \frac{\int_{\delta_j}|\theta_{QSSSC}(x,t) - \theta_{QSS}(x,t)|dt}{\int_{\delta_j}\theta_{QSS}(x,t)dt}100 \\ &= \frac{\int_{\delta_j}|\theta_{decay}(x,t)|dt}{\int_{\delta_j}\theta_{QSS}(x,t)dt}100 \end{aligned} \tag{41}$$

where the integrals are calculated over δ_j, which is the jth on-time. The integration domain is limited to the on-times,

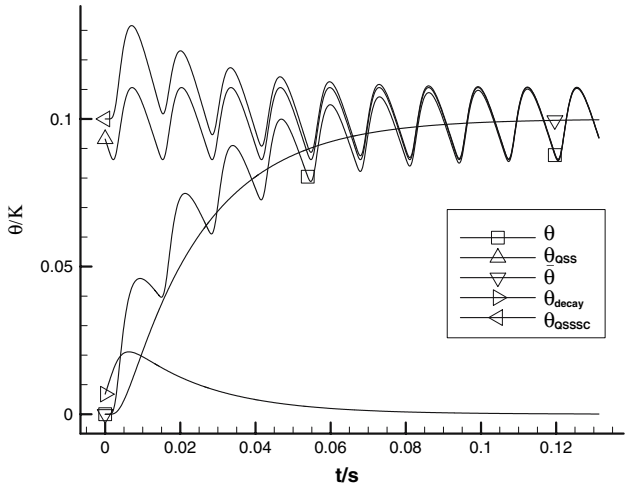

Fig. 3 Temperature evolutions in 1D slab, $\psi = 0$ ($x/H = 0$, $\alpha = 0.1$, $T' = 0.3$, $Bi = 10$)

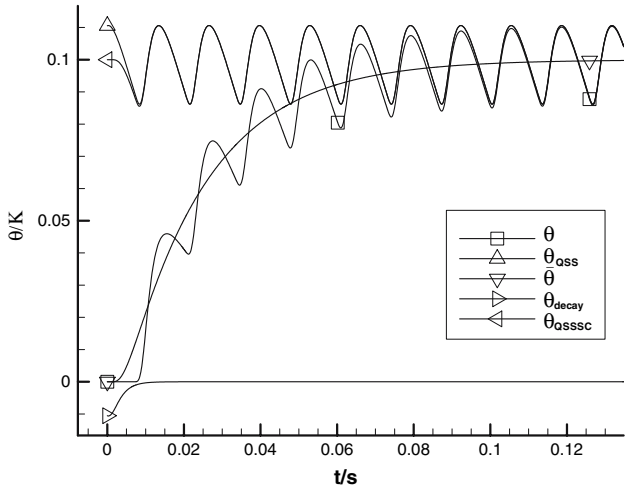

Fig. 4 Temperature evolutions in 1D slab, $\psi = \psi^*$ ($x/H = 0$, $\alpha = 0.1$, $T' = 0.3$, $Bi = 10$)

because this is the only interval of interest when performing calculations for ECM. During the on-time of the pulse, the actual shape change of the workpiece occurs, which is the ultimate goal for simulations in ECM. The states during the off-times are of no primary importance.

A condensed analysis of E will be given in the following. E_j is mainly a function of four dimensionless parameters: Bi, $T' = \frac{\alpha' T}{H^2}$, α and $\frac{x}{H}$. Two additional parameters are the number of on-time j, and ψ. E_1 is shown in Fig. 5 for $\alpha = 0.1$ and $x/H = 0.99$, with $\psi = 0$, and in Fig. 6 for the same setup, but with $\psi = \psi^*$.

One can distinguish three zones A, B and C in Fig. 5. First, there is zone A for $Bi < 1$, where E is function of $\gamma = BiT'$. In this zone, E is independent of x/H, and if $\psi = \psi^*$ is applied, E becomes zero, which is in agreement with the lumped capacity solution from Sect. 4.1.1. For zone A, an analytical expression for E_j can be found,

$$E_j = \frac{(\frac{1-e^{\alpha\gamma}}{e^{\gamma}-1} + \alpha)(1 - e^{-\alpha\gamma})e^{-(j-1)\gamma}}{\alpha\gamma + (1 - \frac{1-e^{\alpha\gamma}}{1-e^{\gamma}})(e^{-\alpha\gamma} - 1)} \tag{42}$$

The maximum value E attains is about 53% (at $BiT' = 2.3$ and $\alpha \to 0$). The second zone, B, starts from $Bi \approx 1$ to higher Bi, where E is function of Bi^2T'. The third zone, C, is reached when Bi becomes large enough, and E is no longer function of Bi. For x/H from 0 to about 0.5, the bell shaped cross section become less high, and shifts slightly to smaller T'. For such values of x/H, zone C starts already at relatively low Bi, and connects almost immediately to zone A. For x/H from about 0.5 to 1, the bell shaped cross section becomes slightly higher again, and shifts strongly to smaller T'. For such values of x/H, zone C is reached at higher Bi numbers, and zone B stretches. For the dependence of E on α, generally one can say, the smaller α, the higher E.

Below the peak in Fig. 5, there is very strong accumulation, and hence averaging is achieved automatically to a certain degree. Above the peak, the effects of all the single pulses are independent of each other and hence averaging is actually not necessary. In both cases $\theta_{\text{decay}}(x,t)$ becomes very small.

The following general conclusions can be drawn from the analysis of the E function. If α is limited to the interval [0.1,1] the worst case values of E can be found in Table 1. It can be seen that the worst case E_1, encountered with $\psi = 0$, is about 187%, which is far from acceptable. Calculating until the second on-time during the QSSSC, we could still encounter a maximum E_2 of 25%, which is still

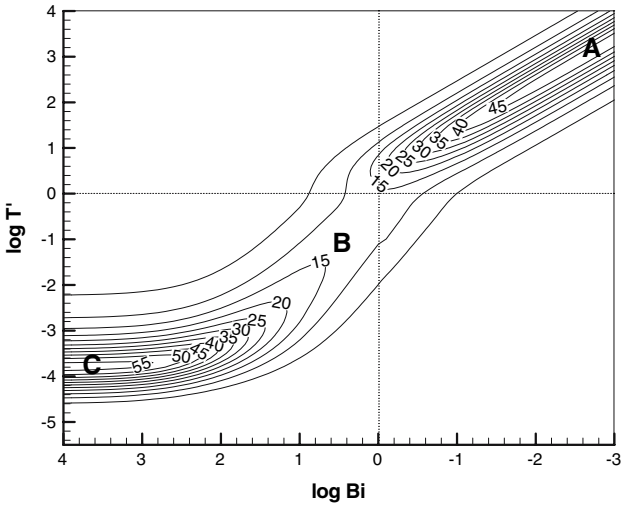

Fig. 5 E_1 as a function of Bi and T', for $\alpha = 0.1$ and $x/H = 0.99$ · $\psi = 0$

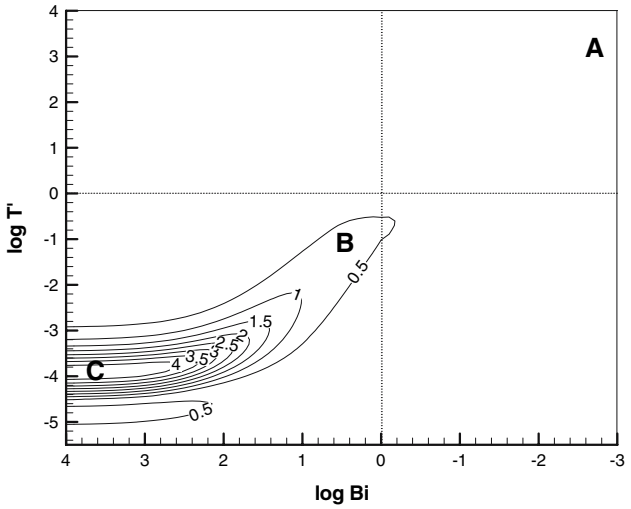

Fig. 6 E_1 as a function of Bi and T', for $\alpha = 0.1$ and $x/H = 0.99$ · $\psi = \psi^*$

unacceptable. By delaying the pulses with $\psi = \psi^*$, the worst case values of E are drastically reduced. It can be seen from Table 1 that the maximum error E_1 is about 5%, which is already acceptable, since in many cases the uncertainties on the thermal parameters of the system are also of this order. Calculating until the second on-time gives a maximum E_2 of about 0.7%, which is already quite satisfactory. This is a worst case scenario, so most cases perform even better than the values from Table 1.

4.2 Convection in the electrolyte

Because in ECM the convection velocity is usually very high, convection is the main mode of transport in the electrolyte. If only convection and bulk heating is considered and the problem is reduced to 1D, Eq. 1 simplifies to a transport equation with a source

$$v\frac{\partial\theta}{\partial x}+\frac{\partial\theta}{\partial t}=\frac{P_{\text{bulk}}}{\rho C_p}=P^*(t) \tag{43}$$

The solution $\theta(x,t)$ in the flow channel is the surface tangent to the characteristic direction vector $(v,1,P^*(t))$ in the (x,t,θ) space, according to [14]. $P^*(t)$ is defined in time as

Table 1 Worst case values of E (minimal value of α:0.1)

ψ	E_1 max	E_2 max
0	187%	25%
ψ^*	5%	0.7%

$$P^*(t)=\begin{cases}0 & \text{for } t'<0\\ P^* & \text{for } iT\le t'<iT+\alpha T, \quad \text{on-time},\\ 0 & \text{for } iT+\alpha T\le t'<(i+1)T, \quad \text{off-time},\end{cases} \tag{44}$$

with $i = 0, 1, 2,...$ the number of the period. Analogously to Sect. 4.1, $t' = t-\psi$ is used to provide the possibility of a time delay ψ.

In addition to obeying Eq. 44, the initial condition $\theta(x,0) = 0$ and the boundary condition $\theta(0,t) = 0$, the solution in the flow channel is shown graphically in Fig. 7 ($\psi = 0$). The duty cycle was $\alpha = 0.3$, which will be used for the rest of this section.

The averaged temperature evolution $\overline{\theta}(x,t)$ is, analogously to the conduction case, calculated by choosing the source term $P^*(t)$ from Eq. 43 equal to the averaged

$$\langle P^*(t)\rangle=\alpha P^* \tag{45}$$

In Fig. 8a, the pulsed case $\theta(x,t)$ (light shade of grey) and averaged case $\overline{\theta}(x,t)$ (transparent dark shade of grey) are shown together. In zone A, there is accumulation of heat in the channel. In zone B, the QSS is partially reached in the flow channel, while in zone C the QSS is fully reached.

The hybrid calculation and the QSSSC can also be performed for this convective system, analogously to the conduction case. In Fig. 9a, the QSS (light shade of grey) and the QSSSC (transparent dark shade of grey) temperature evolutions are both shown. The QSSSC is achieved in zone D, and in zone E the QSSSC becomes equal to the QSS in the first part of the flow channel.

It can be seen in Fig. 8a that by using the averaged temperature to approximate the pulsed temperature, there is a permanent underestimation in zone A. The following decomposition can be made for the transient,

$$\theta(x,t)=\overline{\theta}(x,t)+\tilde{\theta}(x,t)+f(\psi,t) \tag{46}$$

with $\tilde{\theta}(x,t)=f(\psi,t)=0$ for $t<0$. In the case of a hybrid calculation, it can be shown that

$$\theta_{\text{hybrid}}(x,t)=\overline{\theta}(x,t)+\tilde{\theta}(x,t-t^*)+f(\psi,t-t^*) \tag{47}$$

In zone B and C another decomposition can be made for the QSS,

$$\theta(x,t)=\overline{\theta}(x)+\tilde{\theta}'(x,t) \tag{48}$$

where $\overline{\theta}(x)$ is no longer a function of t, and where $\tilde{\theta}'(x,t)$ is a different ripple than $\tilde{\theta}(x,t)$ in Eqs. 46 and 47. The average of the pulsed temperature, in zone B and C, is hence automatically equal to the averaged SS temperature, $\langle\theta(x,t)\rangle=\overline{\theta}(x)$. By using the QSSSC as an approximation for the QSS, it can be seen in Fig. 9a that there was a

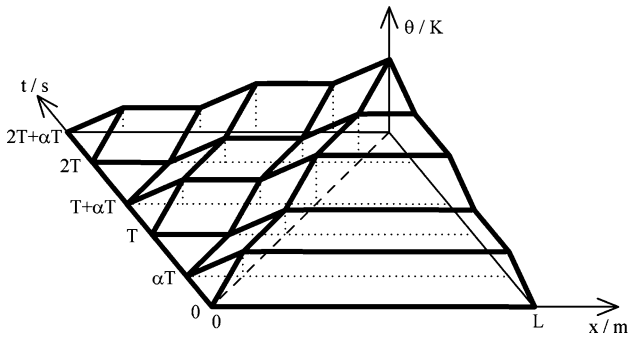

Fig. 7 Graphical solution of the temperature evolution, with convection and bulk heating, as a function of time and space. The characteristic direction is shown in dashed line

permanent overestimation in zone D. Here, the following decomposition can be made,

$$\theta_{\mathrm{QSSSC}}(x,t) = \overline{\theta}(x) + \tilde{\theta}(x,t) + f(\psi,t) \tag{49}$$

Equation 48 is also valid in zone D and E for the QSS. In zone E, the QSSSC becomes equals to the QSS.

If the pulse train is delayed with an interval $\psi = \psi_c^*$, with

$$\psi_c^* = \frac{(1-\alpha)T}{2} \tag{50}$$

$f(\psi,t)$ becomes zero in Eqs. 46, 47 and 49. Hence, in zone A, the average of the pulsed case becomes equal to the averaged temperature, $\langle\theta(x,t)\rangle = \overline{\theta}(x,t)$ (see Eq. 46), see also Fig. 8b. Also, if $\psi = \psi_c^*$, in zone D, the average of the QSSSC becomes equal to the average of the QSS, $\langle\theta_{\mathrm{QSSSC}}(x,t)\rangle = \langle\theta(x,t)\rangle$ (Eqs. 49 and 48), see also Fig. 9b. Although the QSSSC is not exactly equal to the QSS, at least their averages are. If the computational effort can be made, calculations can be performed until the QSS (zone E), for perfect results.

By taking slices from Figs. 8 and 9, a clearer picture can be obtained. Different cases can be considered, which are distinguished by the Strouhal number, defined as

$$St = \frac{L}{vT} \tag{51}$$

If $St \gg 1$, the characteristic direction would lie close to the t-axis in Fig. 7. Slices from Fig. 8a, b would be similar to what is shown in Fig. 10a, b, respectively.

Slices from Fig. 9a, b would be similar to what is shown in Fig. 11a, b, respectively.

If $St \ll 1$, the characteristic direction would lie close to the x-axis in Fig. 7. Slices from Fig. 8a, b would be similar to what is shown in Fig. 12a, b, respectively. Zone A is passed very quickly. Applying a time delay for the pulse train has hardly any consequences in this case.

Slices from Fig. 9a, b would be similar to what is shown in Fig. 13a, b, respectively. In the case with $\psi = \psi_c^*$, the QSSSC during the first on-time is exactly equal to the QSS, $\theta_{\mathrm{QSSSC}}(x,t) = \theta(x,t)$, while in the case with $\psi = 0$, there is a difference. Note that for small St, the best way to calculate the QSS, is actually by pulsing, starting from a state with $\theta(x,t) = 0$. Hence the QSSSC is not the favoured method in this case. However, it is possible that the QSSSC may be applied for other reasons, e.g., conduction with large time constants in the same system.

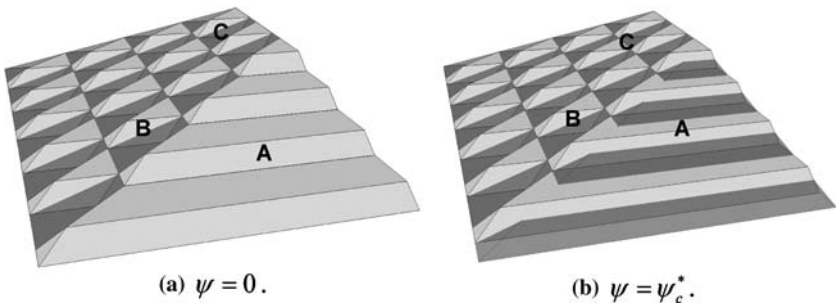

Fig. 8 Pulsed (light shade of grey) and averaged (transparent dark shade of grey) transient temperature evolutions. The quantities on the axes are the same as in Fig. 7

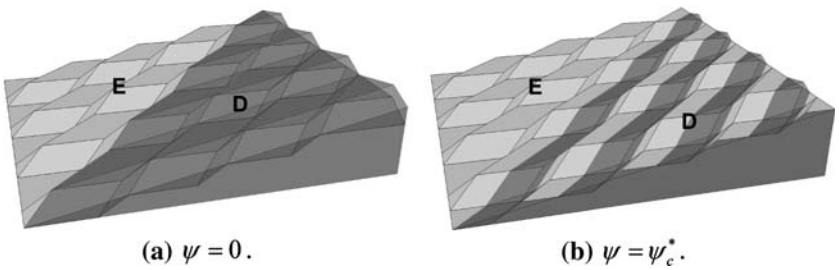

Fig. 9 QSS (light shade of grey) and QSSSC (transparent dark shade of grey) temperature evolutions. The quantities on the axes are the same as in Fig. 7

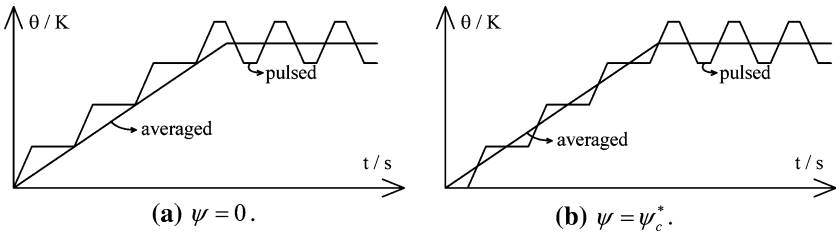

Fig. 10 Transient temperature evolution for large *St*

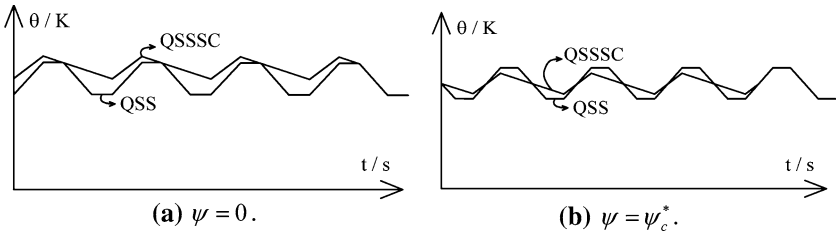

Fig. 11 QSSSC temperature evolution for large *St*

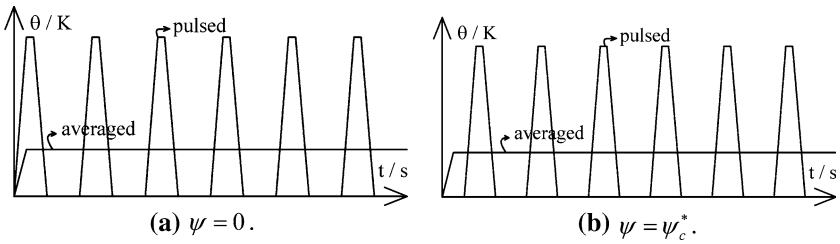

Fig. 12 Transient temperature evolution for small *St*

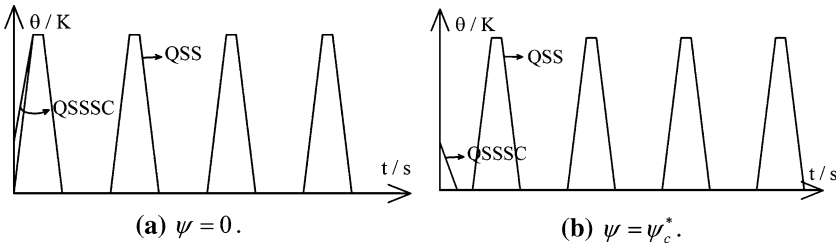

Fig. 13 QSSSC temperature evolution for small *St*

5 Method

If the total machining time is large enough compared to the time scales of the temperature evolution, it is a good approximation to neglect the slow transients and say that the system is always in QSS. This way, the QSSSC provides enough information to know the temperature distribution during the whole machining time. For heat transfer by conduction the following method can be adopted. First the averaged SS is calculated. Afterwards, by delaying the pulses with ψ^*, the QSS can be calculated in numerical calculations by time stepping through the delay interval ψ^*, and the first on-time. This should provide satisfactory predictions of temperature during the on-time (5% error worst case for the simplified model). If a higher accuracy is needed, one has to time step also through the off-time, and the second on-time. The temperature distribution during the second on-time has then at worst 0.7% deviation from the real QSS (for the simplified model). For heat transfer by convection in the flow channel, the optimal results are obtained if the pulses are shifted with ψ_c^*. The heat pulse shifting for convection and conduction have to be taken the same, since in the more general system they result from the same current pulsing. For $T \ll \tau$, $\psi^* \approx \psi_c^*$, hence applying the pulse delay is generally beneficial to the convection and the conduction case.

If the time scales of the temperature evolution are not small enough compared to the total machining time, the hybrid calculation can be used. This method is analogous to the QSSSC above, except that the initial state before applying the pulses is obtained by time stepping. Delaying the pulse on-time ψ^* with is advantageous to minimize $\theta_{\mathrm{decay}}(x,t)$ and calculating more periods will provide more accurate results. The worst case errors are not quantified in this case, and will be higher than with the QSSSC. The hybrid calculation works for the convection case as well

(see Eq. 47), with the optimal pulse delay being ψ_c^*. Note that it is possible that the hybrid calculation is actually a QSSSC for the convection in the flow channel, while this is not the case for the conduction in the electrode, or vice versa, because of the possibly very different time scales.

The method using the hybrid calculation provides one period of data at a time, which is a downside compared to the QSSSC. Another possible method is to calculate the ripple $\tilde{\theta}(x,t)$ (using a QSSSC or a hybrid calculation), and adding this ripple $\tilde{\theta}(x,t)$ to the averaged temperature evolution $\tilde{\theta}(x,t)$. Neglecting $\theta_{\text{decay}}(x,t)$, it is then possible to reconstruct the temperature transient (see Eq. 36).

6 Conclusions

As a general method to solve thermal problems during PECM, the full transient calculation is always an option. However, this method can be computationally very expensive, if not practically impossible, if the full detail of the pulses has to be considered. When the full transient calculation would be too expensive, simplified methods are proposed: the QSSSC, the hybrid calculation and the reconstruction of the temperature transient. These approximate methods can be performed with a minimum of computational effort.

Analytical solutions of simplified sub-problems were analyzed in this work. The assumptions of the models used to derive the analytical solutions are too strict for real life Electrochemical Machining (ECM) conditions. Nevertheless, interesting conclusions can be made. Applying time delays ψ to the pulses during the calculations strongly improves the results of the approximate methods. Analytical expressions for optimal values of ψ are obtained in this work.

References

1. Smets N, Van Damme S, De Wilde D, Weyns G, Deconinck J J Appl Electrochem (submitted)
2. Lohrengel M, Kluppel I, Rosenkranz C, Betterman H, Schultze J (2003) Electrochim Acta 48(20–22):3203
3. Mount A, Clifton D, Howarth P, Sherlock A (2003) J Mater Process Technol 138:449
4. Rajurkar KP, Zhu D, McGeough JA, Kozak J, De Silva A (1999) Ann CIRP 48(2):567
5. Kozak J, Rajurkar K (1991) J Mater Process Technol 28(1–2):149
6. Kozak J (2004) Bull Polish Acad Sci: Tech Sci 52(4):313
7. Datta M, Landolt D (1981) Electrochim Acta 26(7):899
8. Kozak J, Rajurkar K, Lubkowski K (1997) Trans NAMRI/SME XXV:159
9. Clark W, McGeough J (1977) J Appl Electrochem 7:277
10. Loutrel S, Cook N (1973) ASME J Eng Ind 95(B/4):1003
11. Smets N, Van Damme S, De Wilde D, Weyns G, Deconinck J (2007) J Appl Electrochem 37(3):315
12. Lienhard JH IV, Lienhard JH V (2005) A heat transfer textbook, 3rd edn. Phlogiston Press, Cambridge, MA, p 762
13. Carslaw H, Jaeger J (1959) Conduction of heat in solids. Oxford University Press, New York, p 520
14. Strauss W (1992) Partial differential equations: an introduction. J. Wiley & Sons, New York, p 440